Theoretical Study on Acetaldehyde and Ethanol Elimination from the Hydrogenation of $CH_3(O)CCo(CO)_3$

Miquel Solà† and Tom Ziegler*

Department of Chemistry, University of Calgary, Calgary, Alberta, Canada T2N 1N4

Received November 13, 1995⊗

A theoretical study based on density functional theory (DFT) has been carried out on the reaction pathways leading to acetaldehyde and ethanol formation from the hydrogenation of the coordinatively unsaturated $CH_3(O)CCo(CO)_3$ complex (**1**). Hydrogenation of **1** represents the last step of the catalytic hydroformylation process. We have found that, in the H_2-induced acetaldehyde elimination reaction, the energy barrier for the oxidative addition/reductive elimination process is only 36.3 kJ·mol^{-1}. This process is kinetically favored over a σ-bond metathesis pathway involving a four-center transition state with a barrier of 70.4 kJ·mol^{-1}. The possible formation of a hydroxycarbene complex which easily will add hydrogen yielding ethanol and regenerating the $HCo(CO)_3$ catalyst has also been discussed. This hydroxycarbene complex is thermodynamically accessible, although the energy barriers for the reaction pathways leading to its formation are larger than 95.5 kJ·mol^{-1}. On the other hand, the production of ethanol from hydrogenation of acetaldehyde through a hydroxymethyl intermediate has an energy barrier of 42.3 kJ·mol^{-1}. It is concluded that the catalytic generation of alcohols does not proceed via the formation of a hydroxycarbene intermediate but rather through further hydrogenation of the aldehyde molecules.

Introduction

The hydroformylation process converts olefins and synthesis gas to predominantly aldehydes with alcohols[1] and alkanes[2a] as minor products. It involves low-valent cobalt[2] and rhodium complexes[2a,3] as catalysts, and it is carried out on a massive industrial scale. The amount of alcohols produced can be increased by raising the temperature or adding water.[2a,b,4,5]

The overall equation for the formation of propanal from ethylene and CO can be written as:

$$2HCo(CO)_4 + CH_2CH_2 + CO \rightarrow CH_3CH_2CHO + Co_2(CO)_8 \quad (1)$$

The most widely accepted mechanism for the hydroformylation reaction of eq 1 is due to Heck and Breslow[6] and involves five steps;[7−15] see Scheme 1.

Scheme 1

Hydroformylation Mechanism

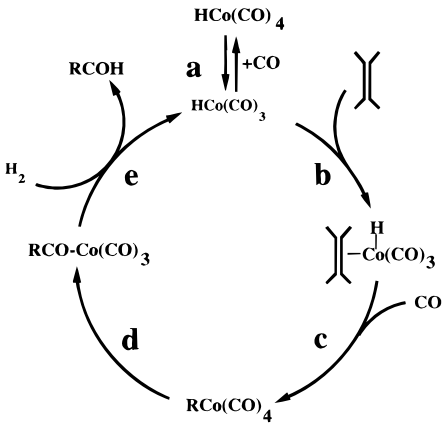

Heck and Breslow, 1962

The active catalyst in Scheme 1 is $HCo(CO)_3$, which is generated from $HCo(CO)_4$ by loss of a CO ligand, step **a** of Scheme 1. Evidence for the presence of $HCo(CO)_3$

† Permanent address: Institut de Química Computacional and Departament de Química, Universitat de Girona, 17071 Girona, Catalonia, Spain.

⊗ Abstract published in *Advance ACS Abstracts,* May 1, 1996.

(1) Rathke, J. W.; Klinger, R. J.; Krause, T. R. *Organometallics* **1991**, *10*, 1350.

(2) (a) Süss-Fink, G.; Meister, G. *Adv. Organomet. Chem.* **1993**, *35*, 41. (b) Orchin, M. *Acc. Chem. Res.* **1981**, *14*, 259. (c) Orchin, M.; Rupilius, W. *Catal. Rev.* **1972**, *6*, 85.

(3) (a) Pino, P.; Piacenti, F.; Bianchi, M. In *Organic Synthesis via Metal Carbonyls*; Wender, I., Pino, P., Eds.; New York, 1977; Vol. II, pp 43−135. (b) Polo, A.; Claver, C.; Castillón, S.; Ruiz, A.; Bayón, J. C.; Real, J.; Mealli, C.; Masi, D. *Organometallics* **1992**, *11*, 3525. (c) Alvila, L.; Pakkanen, T. A.; Pakkanen, T. T.; Krause, O. *J. Mol. Catal.* **1992**, *73*, 325. (d) Reus, S. I.; Kamalov, G. L.; Golodets, G. I. *Kinet. Catal.* **1991**, *32*, 694. (e) Crudden, C. M.; Alper, H. *J. Org. Chem.* **1994**, *59*, 3091.

(4) (a) Masters, C. *Adv. Organomet. Chem.* **1979**, *17*, 61. (b) Feder, H. M.; Rathke, J. W. *Ann. N.Y. Acad. Sci.* **1980**, *333*, 45.

(5) Bartik, T.; Bartik, B.; Hanson, B. E. *J. Mol. Catal.* **1993**, *85*, 121.

(6) (a) Heck, R. F.; Breslow, D. S. *J. Am. Chem. Soc.* **1961,** *83*, 4023. (b) Heck, R. F. *Acc. Chem. Res.* **1969**, *2*, 10.

(7) (a) Versluis, L.; Ziegler, T.; Baerends, E. J.; Ravenek, W. *J. Am. Chem. Soc.* **1989**, *111*, 2018. (b) Versluis, L.; Ziegler, T. *Organometallics* **1990**, *9*, 2985. (c) Versluis, L.; Ziegler, T.; Fan, L. *Inorg. Chem.* **1990**, *29*, 4530. (d) Versluis, L.; Ziegler, T. *J. Am. Chem. Soc.* **1990**, *112*, 6763. (e) Ziegler, T.; Cavallo, L.; Bérces, A. *Organometallics* **1992**, *12*, 3586.

(8) Wermer, P.; Ault, B. S.; Orchin, M. *J. Organomet. Chem.* **1978**, *162*, 189.

(9) Ungváry, F.; Markó, L. *J. Organomet. Chem.* **1969**, *20*, 205.

(10) (a) Pino, P. *Ann. N.Y. Acad. Sci.* **1983**, *415*, 111. (b) Orchin, M. *Ann. N.Y. Acad. Sci.* **1983**, *415*, 129. (c) Ungváry, F.; Sisak, A.; Markó, L. *Adv. Chem. Ser.* **1990**, *No. 230*, 297.

(11) Klinger, R. J.; Rathke, J. W. *J. Am. Chem. Soc.* **1994**, *116*, 4772.

(12) Folga, E.; Ziegler, T. *J. Am. Chem. Soc.* **1993**, *115*, 5169.

(13) Klinger, R. J.; Rathke, J. W. *Inorg. Chem.* **1992**. *31*, 804.

S0276-7333(95)00881-8 CCC: $12.00

Scheme 2

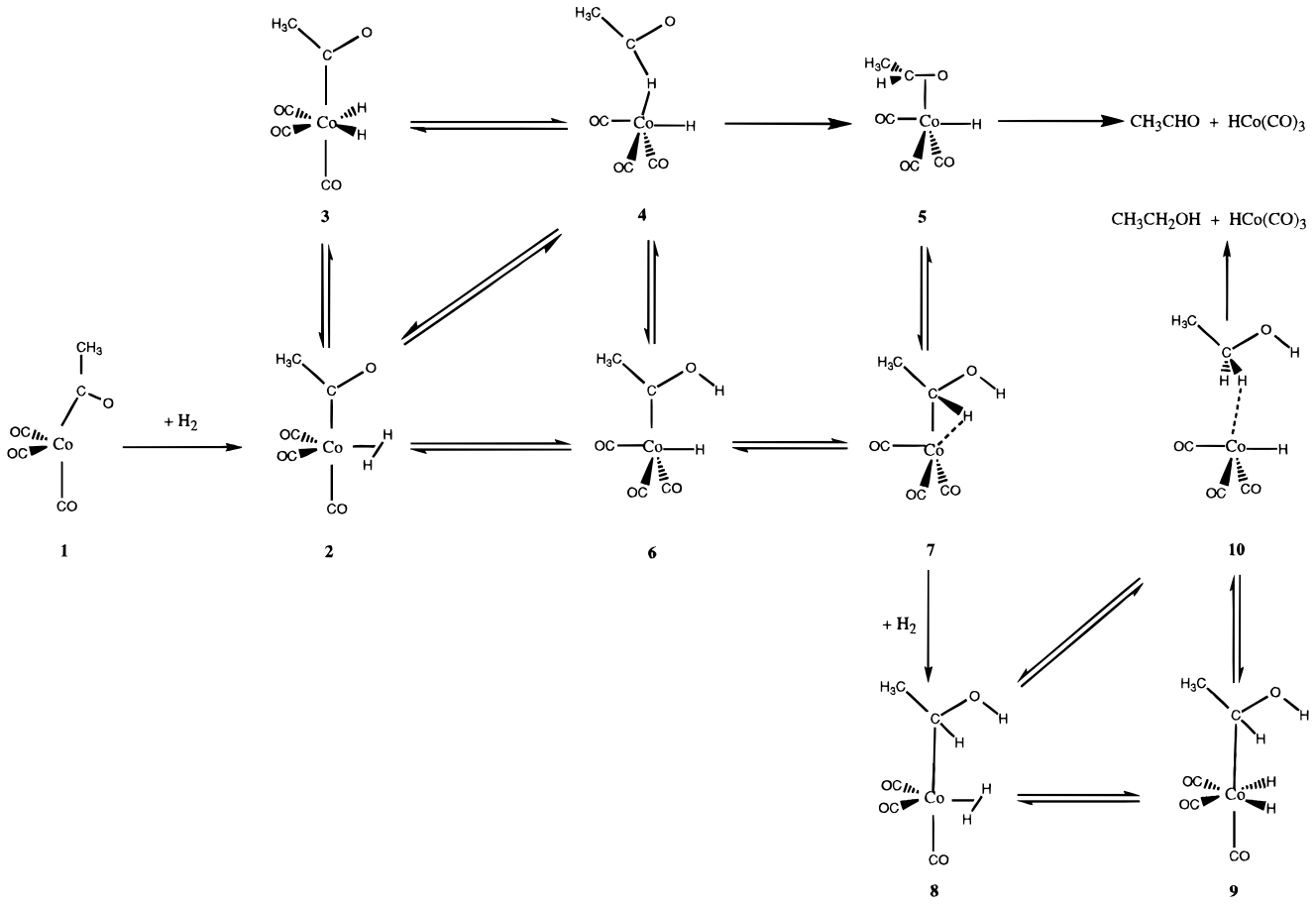

has been provided by matrix isolation techniques.[8] A kinetic study by Ungváry and Markó indicated further that $HCo(CO)_4$ is about 0.3% dissociated to $HCo(CO)_3$ at room temperature.[9]

The focus of the present study is on the final elimination of aldehyde, step **e** of Scheme 1. In this step H_2 is assumed to add oxidatively to the unsaturated acyl complex yielding a dihydro acyl species

$$R(O)CCo(CO)_3 + H_2 \rightarrow R(O)CCo(CO)_3(H)_2 \quad (2)$$

followed by an irreversible reductive elimination of the aldehyde molecule:

$$R(O)CCo(CO)_3(H)_2 \rightarrow RCHO + HCo(CO)_3 \quad (3)$$

Oxidative addition (eq 2) and reductive elimination (eq 3) are common elementary reaction steps among late transition metals such as cobalt. However, aldehyde elimination could alternatively proceed directly through the formation of a four-center transition state in a σ-bond metathesis process. The activation of H−H and C−H linkages by σ-bond metathesis is a well-established process among electron-poor early transition metals[7b,16] and it has been invoked for late transition metals as well. The first objective of our study will be to examine aldehyde elimination by H_2 for both pathways. A previous theoretical investigation[7b] on this subject was inconclusive since it made use of limited geometry optimization.

The other point we want to address is also connected to step **e** of Scheme 1. It is concerned with possible pathways leading to alcohol formation as a side reaction in the hydroformylation process. Alcohol formation is normally assumed[2a,10c,17] to result from further reaction of the aldehyde formed in step **e** with the catalyst $HCo(CO)_3$ to form a hydroxyalkyl complex

$$HCo(CO)_3 + RC(O)H \rightarrow R(OH)(H)CCo(CO)_3 \quad (4)$$

which can react with H_2 to eliminate the alcohol and regenerate the catalyst $HCo(CO)_3$:

$$R(OH)(H)CCo(CO)_3 + H_2 \rightarrow RCH_2OH + HCo(CO)_3 \quad (5)$$

Some authors[4a,18] have suggested an alternative mechanism. This mechanism involves hydroxycarbene as an intermediate. It is suggested that hydroxycarbene is formed in step **e** of Scheme 1 by a hydride transfer to the acyl oxygen rather than the acyl carbon:

(14) Pino, P.; Major, A.; Spindler, F.; Tannenbaum, R.; Bor, G.; Horváth, T. *J. Organomet. Chem.* **1991**, *417*, 65.
(15) (a) Harrod, J. F.; Yorke, W. J. *Inorg. Chem.* **1981**, *20*, 1156. (b) Sweany, R. L.; Russell, F. N. *Organometallics* **1988**, *7*, 719. (c) Li, J.; Dickson, R. M.; Ziegler, T. *J. Am. Chem. Soc.* **1995**, *117*, 11482.
(16) (a) Ziegler, T.; Folga, E.; Berces, A. *J. Am. Chem. Soc.* **1993**, *115*, 636. (b) Burger, B. J.; Thompson, M. E.; Cotter, W. D.; Bercaw, J. E. *J. Am. Chem. Soc.* **1990**, *112*, 1566. (c) Thompson, M. E.; Buxter, S. M.; Bulls, A. R.; Burger, B. J.; Nolan, M. C.; Santarsiero, B. D.; Schaefer, W. P.; Bercaw, J. E. *J. Am. Chem. Soc.* **1987**, *109*, 203. (d) Watson, P. L.; Parshall, G. W. *Acc. Chem. Res.* **1985**, *18*, 51. (e) Davis, J. A., Watson, P. L., Liebman, J. F., Greenberg, A., Eds. *Selective Hydrocarbon Activation*; VCH Publishers: New York, 1990.
(17) Fahey, D. R. *J. Am. Chem. Soc.* **1981**, *103*, 136.
(18) Nicholas, K. M. *Organometallics* **1982**, *1*, 1713.

$$R(O)CCo(CO)_3(H)_2 \rightarrow R(OH)CCo(CO)_3H \quad (6)$$

Further isomerization of the hydroxycarbene complex will produce the hydroxyalkyl complex

$$R(OH)CCo(CO)_3H \rightarrow R(OH)(H)CCo(CO)_3 \quad (7)$$

which again can react with H_2 to eliminate $HCo(CO)_3$ and an alcohol according to eq 5.

We shall here investigate the processes in eqs 4 and 5 as well as the alternative mechanism of eqs 6, 7, and 5. The alternative route toward alcohol formation has not been studied previously in any details, probably because there are little experimental data on hydroxycarbenes in the literature. To our knowledge, only a single rhenium hydroxycarbene[19] is known. On the other hand, several methoxycarbene complexes have been characterized.[19,20]

Our theoretical investigation will be based on density functional theory (DFT). The application of approximate density functional theory to organometallic chemistry has been reviewed recently.[7,12,16a,21]

Computational Details

The reported calculations were carried out by using the Amsterdam density functional (ADF) program system, developed by Baerends *et al.*[22] and vectorized by Ravenek.[23] The numerical integration scheme employed was that of te Velde and Baerends.[24] An uncontracted triple-ζ basis set[25] was used for describing the 3s, 3p, 3d, 4s, and 4p orbitals of cobalt. For carbon (2s,2p), oxygen (2s,2p), and hydrogen (1s), double-ζ basis sets[25] were employed and augmented by an extra polarization function. Electrons in lower shells were treated within the frozen core approximation.[22a] A set of auxiliary s, p, d, f, and g functions,[26] centered in all nuclei, was introduced in order to fit the molecular density and Coulomb potential accurately in each SCF cycle. All geometry optimizations and energy differences were computed including nonlocal corrections (Becke's nonlocal exchange correction[27] and Perdew's nonlocal correlation correction[28]). The geometry optimization procedure was based on a method developed by Versluis and Ziegler.[29] All reaction paths were followed by a linear transit procedure in which an internal coordinate (a bond length) was chosen as the reaction coordinate. Small steps of 0.025 Å were taken along the transit. At each point of the linear transit path the rest of the internal coordinates were fully optimized. The energy profile obtained in this way does not represent the intrinsic reaction path but rather set an upper energy limit for the activation barrier of the process. Certainly, these linear transits are not optimal, but they contain the essential features of the intrinsic reaction paths and ensure that the approximate transition state found actually connects with the reactant and product for the process under investigation. No symmetry constraints were imposed on minima and during the linear transit optimizations. In ligand addition or dissociation processes only the thermodynamics of the process was analyzed.

Results and Discussion

The starting point for our discussion is the acyl intermediate $CH_3(O)CCo(CO)_3$. It is shown as **1** in Scheme 2. The reaction of **1** with H_2 can lead to formation of aldehyde and regeneration of the catalyst $HCo(CO)_3$, **2** → **5** of Scheme 2. Alternatively, **1** can react with two molecules of H_2 to form alcohol and $HCo(CO)_3$, **2** → **10** of Scheme 2. We turn first to the process in which acetaldehyde is formed from the interaction of $CH_3(O)CCo(CO)_3$ (**1**) with molecular hydrogen.

H_2-Induced Acetaldehyde Elimination from $CH_3(O)CCo(CO)_3$. Optimized key structures for the aldehyde forming process are depicted in Figure 1. Table 1 gathers the relative energies of minima and approximate transition states (TS) obtained from the linear transit procedures.

The most stable structure[7b] for the reactant $CH_3(O)CCo(CO)_3$, (**1**), was found to have the acyl group in the axial position, Figure 1. In this structure, there is a marked η^2 interaction between a lone pair on the acyl oxygen and the coordinatively unsaturated metal center.

1a **1b**

The reaction of **1** with H_2 results in the dihydrogen complex $CH_3(O)CCo(CO)_3(\eta^2\text{-}H_2)$. Complex **2** with H_2 in an equatorial site and the hydrogen−hydrogen vector perpendicular to the $Co-C_{acyl}$ bond was found to be the conformation of lowest energy.[7b] In this conformation, the empty $\sigma^*_{H_2}$ orbital has the correct orientation to interact with the HOMO[7b] **1a** of complex **1** and the occupied σ_{H_2} orbital can interact with the LUMO[7b] **1b**. Electron donation to the $\sigma^*_{H_2}$ orbital leads to the activation of molecular hydrogen which has a larger H−H bond distance in the η^2 adduct (0.826 Å) than in the free H_2 molecule (0.755 Å). The dihydrogen complex **2** is more stable than **1** + H_2 by 10.5 kJ·mol^{-1}. Interestingly, the $Co-C_{acyl}$ bond distance is increased by 0.2 Å in **2** compared to **1**. The weaker bond in **2** will facilitate aldehyde elimination in a subsequent step.

It is generally assumed that the aldehyde elimination step proceeds from **2** by oxidative addition of the η^2-H_2 ligand to form the dihydride complex, **3**. We find the addition process **2** → **3** to be endothermic by 25.8 kJ·mol^{-1}. This is in agreement with the experimental fact that, in a similar complex, the predominant intermediate observed is **2** rather than **3**.[15b] It is worth noting that the nature of the ancilary ligands may change the relative energy of the dihydrogen complex

(19) Wong, W. K.; Tam, W.; Gladysz, J. A. *J. Am. Chem. Soc.* **1979**, *101*, 5440.

(20) (a) Farnell, L. F.; Randall, E. W.; Rosenberg, E. *Chem. Commun.* **1971**, 1078. (b) Casey, C. P.; Neumann, S. M. *J. Am. Chem. Soc.* **1977**, *99*, 1651.

(21) (a) Ziegler, T. *Chem. Rev.* **1991**, *91*, 651. (b) Ziegler, T. *Pure Appl. Chem.* **1991**, *63*, 873. (c) Ziegler, T.; Versluis, L. *Adv. Chem. Res. Ser.* **1992**, *No. 230*, 75. (d) Ziegler, T. *NATO ASI Ser.* **1992**, *C367*, 357. (e) Ziegler, T. *Can. J. Chem.* **1995**, *73*, 743.

(22) (a) Baerends, E. J.; Ellis, D. E.; Ros, P. *Chem. Phys.* **1973**, *2*, 41. (b) Baerends, E. J. Ph.D. Thesis, Vrije Universiteit, Amsterdam, 1975.

(23) Ravenek, W. In *Algorithms and Applications on Vector and Parallel Computers*; te Riele, H. J. J., Dekker, Th. J., van de Vorst, H. A., Eds.; Elsevier: Amsterdam, 1987.

(24) te Velde, G.; Baerends, E. J. *J. Comp. Phys.* **1992**, *99*, 84.

(25) (a) Snijders, G. J.; Baerends, E. J.; Vernooijs, P. *At. Nucl. Data Tables* **1982**, *26*, 483. (b) Vernooijs, P.: Snijders, G. J.; Baerends, E. J. *Slater Type Basis Functions for the Whole Periodic System*; Internal Report; Vrije Universiteit of Amsterdam: Amsterdam, The Netherlands, 1981.

(26) Krijn, J.; Baerends, E. J. *Fit functions in the HFS method*; Internal Report (in Dutch); Vrije Universiteit of Amsterdam: Amsterdam, The Netherlands, 1984.

(27) Becke, A. D. *Phys. Rev. A* **1988**, *38*, 2398.

(28) Perdew, J. P. *Phys. Rev. B* **1986**, *33*, 8822.

(29) Versluis, L.; Ziegler, T. *J. Chem. Phys.* **1988**, *88*, 322.

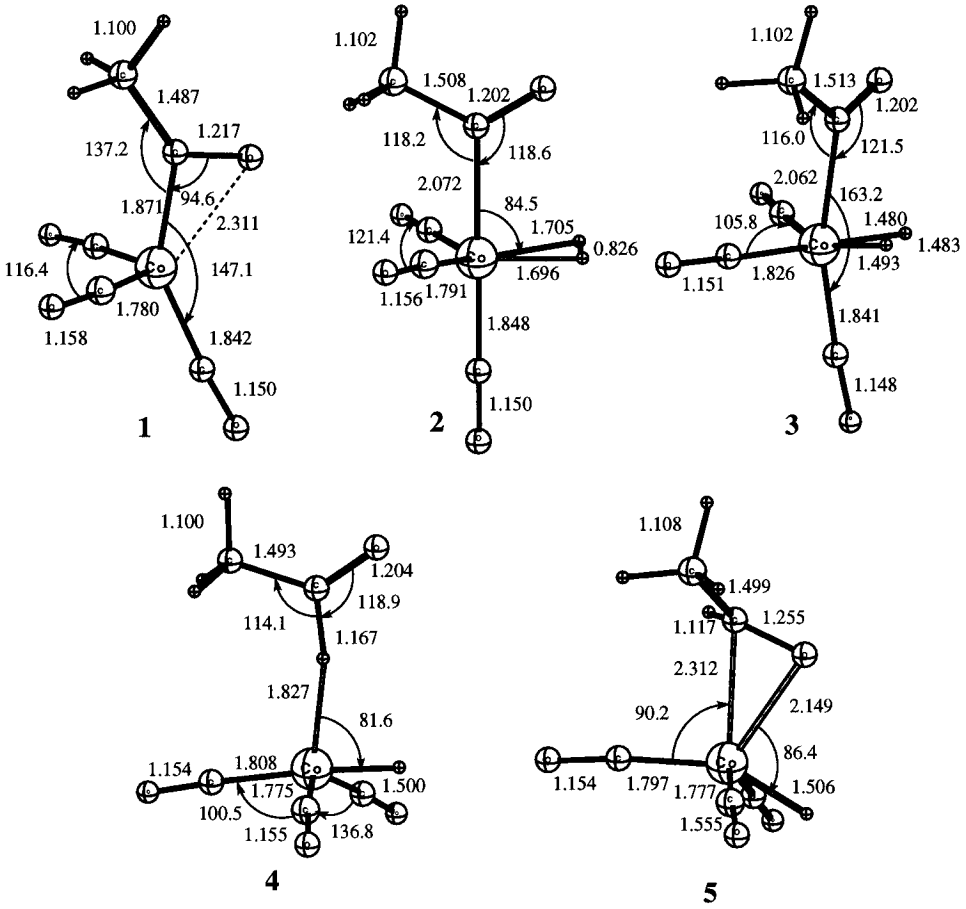

Figure 1. Optimized structures for complexes **1**−**5**. Bond distances are in Å, and angles are in deg.

Table 1. Relative Energies[a] for Species Involved in the H_2-Induced Aldehyde Elimination Process

species	rel energy[a]	species	rel energy[a]
1 + H_2	10.5	TS(**3** → **4**)[b]	36.3
2	0	TS(**2** → **4**)[b]	70.4
3	25.8	TS(**2** → **6**)[b]	95.5
4	14.0	TS(**4** → **6**)[b]	186.0
5	6.1	TS(**5** → **7**)[b]	48.4
6	33.2	TS(**6** → **7**)[b]	39.8
7	−5.0	CH_3CHO + $HCo(CO)_3$	41.1
TS(**2** → **3**)[b]	30.5		

[a] All energies in kJ·mol^{-1}are relative to **2**. [b] The energy of the approximate transition state TS(**a** → **b**) is taken from the highest energy point on the linear transit **a** → **b**.

compared to its dihydride isomer. Thus, substitution of CO by PR_3 leads to a stabilization of complex **3** compared to **2**.[7b] The position of the transition metal center within a triad may also affect the relative stability of the dihydrogen and dihydride species. Calculations have shown[15c] that the stability of the dihydride isomer increases in comparison to the dihydrogen adduct in going from the 3d (Co) and 4d (Rh) congeners to the 5d (Ir) homologue. This trend is caused by relativistic effects[15c] which become important for 5d transition elements.

Figure 2 depicts the energy profiles for the paths connecting complexes **2** to **7**. The activation barrier for **2** → **3** is only 30.5 kJ·mol^{-1}. Such a low energy barrier is in agreement with previous kinetic studies in related complexes.[15a] At the highest point along the transit the H−H bond length is 1.298 Å, the transition state being product-like; see TS(**2** → **3**) of Figure 3. This low energy barrier can be attributed to the aforementioned favorable interactions along the transit of the σ_{H_2} and $\sigma^*_{H_2}$ orbitals with the LUMO **1b** and HOMO **1a** of complex **1**, respectively.

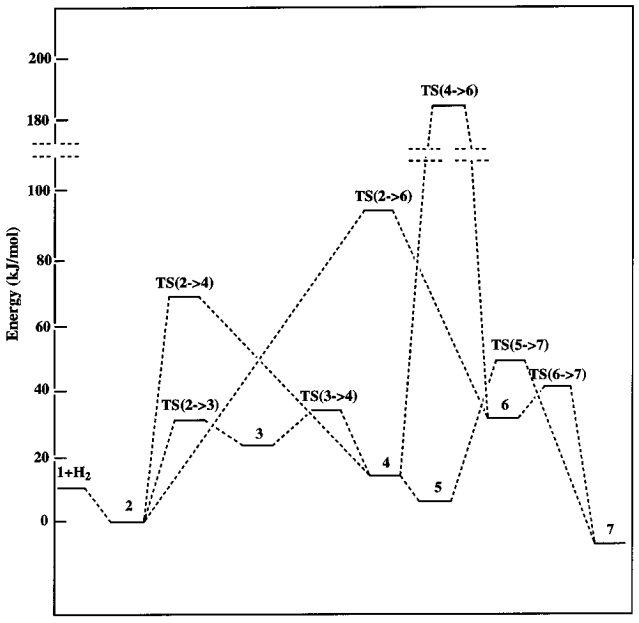

Figure 2. Energy profile for the paths connecting complexes **2**−**7**. The energy zero point refers to structure **2**. The H−H bond distance represents the reaction coordinate.

The elimination of $CH_3C(O)H$ from **1** by H_2 gives rise to the adduct **4,** where acetaldehyde is complexed to the $HCo(CO)_3$ fragment through the hydrogen of the carbonyl carbon in an agostic[30] interaction. The Co−H distance of 1.827 Å is only 0.3 Å longer than a normal

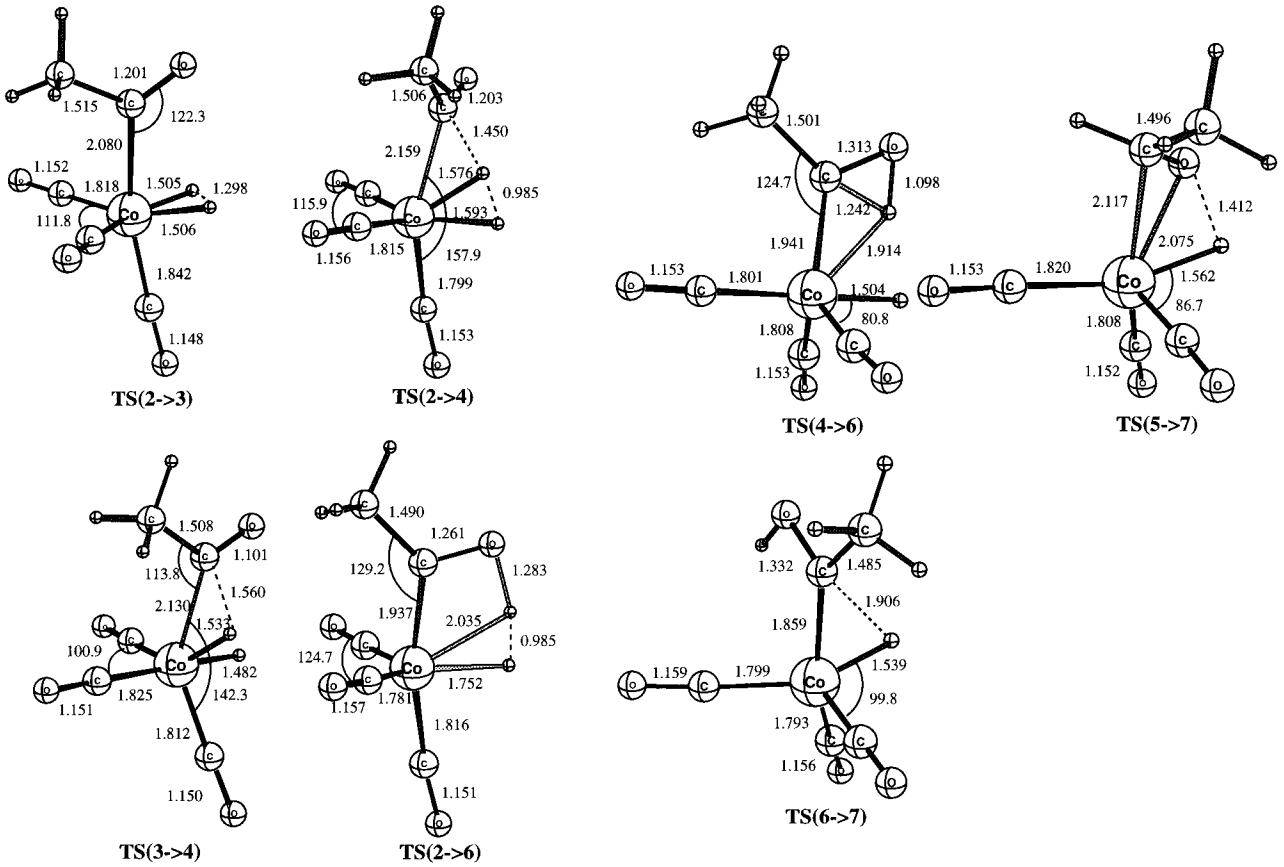

Figure 3. Structures of approximate transition states obtained from linear transits.

Co−H bond, and the C−H distance is stretched to 1.167 Å. Complex **4** is 14.0 kJ·mol^{-1} less stable than complex **2**, and 27.1 kJ·mol^{-1} more stable than acetaldehyde and $HCo(CO)_3$. However, it must be noted that the final elimination of acetaldehyde will be facilitated by the formation of $HCo(CO)_4$ as CO adds to the $HCo(CO)_3$ species. This process was found to be highly exothermic by 169 kJ·mol^{-1}.[7e]

As mentioned in the Introduction, complex **4** could conceivably be formed through an oxidative addition/reductive elimination path (**2** ⇀ **3** ⇀ **4**) or alternatively in a process involving a four-center transition state which avoids direct oxidative addition of H_2 to the metal center (**2** ⇀ **4**). The total activation energy found for the **2** ⇀ **3** ⇀ **4** path is 36.3 kJ·mol^{-1} with the barrier for the oxidative addition step **2** ⇀ **3**, Figure 2, given by 30.5 kJ·mol^{-1} and that of the reductive elimination step **3** ⇀ **4** given by 10.5 kJ mol^{-1}. Thus, for the path **2** ⇀ **3** ⇀ **4** the oxidative addition is the crucial step. The approximate transition state for the reductive elimination path, TS(**3** ⇀ **4**) of Figure 3, has a stretched C−H bond of 1.560 Å coordinated in a way similar to the H−H bond of **2** and TS(**2** ⇀ **3**). Also in a way similar to TS(**2** ⇀ **3**), the σ_{CH} and σ^*_{CH} orbitals can interact stabilizing with **1b** and **1a**, respectively, of the fragment **1**. These interactions stabilize considerably the transition state TS(**2** ⇀ **3**) by affording relatively strong Co−H and Co−C(O)CH_3 bonds with distances similar to those in the reactant **3**.

The activation barrier for the σ−bond metathesis path **2** ⇀ **4** is 70.4 kJ·mol^{-1}. Thus, the oxidative addition/reductive elimination step is favored by 34.1 kJ·mol^{-1} in terms of activation energy. The approximate transition state for the **2** ⇀ **4** reaction is shown as TS(**2** ⇀ **4**) in Figure 3. It exhibits a stretched H−H bond at 0.985 Å, indicating that H_2 activation as for the alternative path **2** ⇀ **3** ⇀ **4** is the crucial part of the reaction. However, in TS(**2** ⇀ **4**) the H−H bond has to be perpendicular to the HOMO **1a** of the fragment **1** in order to produce a C−H bond. Thus, the $\sigma^*_{H_2}$ orbital cannot be stabilized by **1a**. Instead $\sigma^*_{H_2}$ interacts with the Co−C(O)CH_3 σ-bonding orbital, **1c**. Unfortunately, the Co−C(O)CH_3 σ-bonding orbital is of lower energy than **1a** and forms in addition a smaller overlap with $\sigma^*_{H_2}$. For this reason the stabilization of $\sigma^*_{H_2}$ is much poorer in TS(**2** ⇀ **4**) than in TS(**2** ⇀ **3**) and the activation energy accordingly higher for breaking the H−H bond.

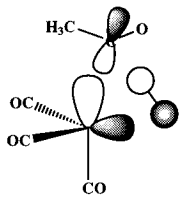

1c

It is worth to note that the CO ligands of the distorted octahedral complexes **2** and **3** rearrange along the transit to **4**, so as to place the hydride in an axial position. In this way the $HCo(CO)_3$ framework regains its most stable conformation.[7e] Adduct **4** can be viewed as a trigonal bipyramid (TBP) species with the aldehyde attached via a C−H σ-bond to the metal center. In the σ-complex, **4**, the aldehyde ligand is in an equatorial

(30) Brown, R. K.; Williams, J. M.; Schultz, A. J.; Stucky, G. D.; Ittel, S. D.; Harlow, R. L. *J. Am. Chem. Soc.* **1980**, *102*, 981.

position and density is donated from the σ_{CH} orbital to the LUMO **1b**. In some ways **4** is similar to an η^1 conformation of the dihydrogen complex **2** in which H_2 is bound end-on.

The σ-complex **4** can rearrange by a simple rotation of the acetaldehyde fragment to the π-complex **5**, which is more stable than **4** by only 7.9 kJ/mol. There are a number of possible conformations for the aldehyde π-complex, of which structures with CH_3CHO in the axial position were found to be less stable than those with the aldehyde coordinated at an equatorial site.[7d] Here, we have considered only the equatorial coordination with the CO bond of CH_3CHO parallel to the H−Co−CO axis of the TBP framework and with the oxygen atom of the CH_3CHO fragment close to the hydride coordinated to cobalt. In complex **5** there is an η^2 interaction in which the π_{CO} and π^*_{CO} of acetaldehyde interact with the metal center in a way similar to σ_{H_2} and $\sigma^*_{H_2}$, respectively, of the η^2-H_2 complex **2**.[31] The C−O bond of the aldehyde is seen to be elongated as a result of the donation of charge from the cobalt center to the π^*_{CO} orbital. Finally, it is worth noting that the Co-O bond length is shorter than the Co−C bond length as experimentally found in similar complexes.[32]

It has been suggested[10b,c] that the hydrogen used in aldehyde elimination comes from the strong acidic $HCo(CO)_4$ species which is present as a precatalyst in significant quantities[10b,c] rather than from H_2 as assumed in step **e** of Scheme 1. According to this mechanism, $HCo(CO)_4$ interacts with the unsaturated $R(O)CCo(CO)_3$ complex and transfers its hydrogen to form the aldehyde and $Co_2(CO)_7$:

$$R(O)CCo(CO)_3 + HCo(CO)_4 \rightarrow RCHO + Co_2(CO)_7 \quad (8)$$

The latter unsaturated species adds subsequently a CO molecule:

$$Co_2(CO)_7 + CO \rightarrow Co_2(CO)_8 \quad (9)$$

The $Co_2(CO)_8$ dimer finally reacts with H_2 to regenerate $HCo(CO)_4$.[1,2b,12,13] Similar steps have been invoked in the homologation of alcohols[33] and in the reduction of aldehydes.[10c]

An elegant experiment[14] based on IR spectroscopy has been designed in order to determine the source of hydrogen in the aldehyde elimination step. The experiment was carried out under normal hydroformylation conditions with hydrogen gas replaced by a mixture of H_2 and D_2. It was established in this study that H_2 is the main source of hydrogen in the aldehyde elimination step, even in the presence of large amounts of $HCo(CO)_4$. The hydride $HCo(CO)_4$ was found to be responsible for only 5% of the hydrogen present in the synthesized aldehydes. We have as a result not considered the elimination path given in eqs 8 and 9.

H_2-Induced Ethanol Elimination from $CH_3(O)CCo(CO)_3$ via Hydroxycarbene Complex Formation and via Further Hydrogenation of Acetaldehyde. We have in the previous section studied the transfer of hydrogen from complexes **2** and **3** to the coordinated carbon atom of the acyl group. One might wonder whether an alternative transfer to the oxygen atom of the acyl group would not be feasible as well. Such a transfer will result in the hydroxycarbene complex **6** of Scheme 2. This species is interesting since it could isomerize further to the hydroxymethyl complex **7** by hydride transfer from the metal center to the carbene carbon. The hydroxymethyl complex **7** can lead to generation of alcohol[2a,10c,17] in the sequence of steps **7** → **8** → **9** → **10** or **7** → **8** → **10**, as illustrated in Scheme 2.

Alcohol formation is one of the important side reactions observed in connection with hydroformylation. It is normally attributed[2a,10c,17] to a further reaction of the aldehyde eliminated in step **e** of Scheme 1 with the catalyst $HCo(CO)_3$ and H_2. More specifically, aldehyde can complex to $HCo(CO)_3$, **5** of Scheme 2, followed by hydride transfer to form a hydroxymethyl complex, **7**. After formation of **7**, alcohol is formed in the sequence of steps mentioned above.

This section is concerned with alcohol formation as a side reaction in the hydroformylation process. It is clear from Scheme 2 that the hydroxymethyl complex **7** must be a key intermediate in this process and that **7** might be formed from the aldehyde adduct **5** as well as the dihydrogen complex **2** via the hydroxycarbene **6**. We shall examine both pathways toward **7** as well as the further conversion of this species to alcohol.

This kinetic investigation was prompted by the fact that we find aldehyde formation

$$CH_3(O)CCo(CO)_3 + H_2 \rightarrow CH_3CHO + HCo(CO)_3 \quad (10)$$

to be a slightly endothermic reaction with a reaction enthalpy of 30.6 kJ·mol^{-1} whereas alcohol formation

$$CH_3(O)CCo(CO)_3 + 2H_2 \rightarrow CH_3CH_2OH + HCo(CO)_3 \quad (11)$$

is exothermic by −39.3 kJ·mol^{-1}. Yet, only aldehyde is formed in large quantities under normal hydroformylation conditions.

We begin by discussing the formation of **7** from **2** via the hydroxycarbene **6**. Table 1 gathers the energies of complexes **6** and **7** relative to **2**. Also given are the activation energies for the pathways leading to **6** and **7**. The molecular structures of complexes **6** and **7** are depicted in Figure 4.

It follows from Table 1 that the hydroxycarbene **6** is only 33.2 kJ·mol^{-1} above **2** in energy, and so it is accesible from a thermodynamic point of view. We have analyzed its possible formation from complexes **2**−**4**.

The reaction path corresponding to the **2** → **6** interconversion has an energy barrier of 95.5 kJ·mol^{-1}. Thus, this process is not likely to take place at room temperature. The transition state for the **2** → **6** interconversion is shown in Figure 3 as TS(**2** → **6**). It exhibits as for TS(**2** → **4**) a stretched H−H bond perpendicular to the plane holding the HOMO **1a**. Therefore the stabilization of the $\sigma^*_{H_2}$ orbital is of the

(31) (a) Dewar, M. J. S. *Bull. Soc. Chim. Fr.* **1951**, *18*, C71. (b) Chatt, J.; Ducanson, J. S. *J. Chem. Soc.* **1953**, 2939.

(32) (a) Buhro, W. E.; Patton, A. T.; Strouse, C. E.; Gladysz, J. A.; McCormick, F. B.; Etter, M. C. *J. Am. Chem. Soc.* **1983**, *105*, 1056. (b) Clark, G. R.; Headford, C. E. L.; Marsden, K.; Roper, W. R. *J. Organomet. Chem.* **1982**, *231*, 335. (c) Gambarotta, S.; Floriani, C.; Chiesi-Villa, A.; Guastini, C. J. *J. Am. Chem. Soc.* **1985**, *107*, 2985. (d) Gambarotta, S.; Floriani, C.; Chiesi-Villa, A.; Guastini, C. J. *J. Am. Chem. Soc.* **1982**, *104*, 2019. (e) Floriani, C. *Pure Appl. Chem.* **1983**, *55*, 1.

(33) Dombeck, B. D. *Adv. Catal.* **1983**, *32*, 325.

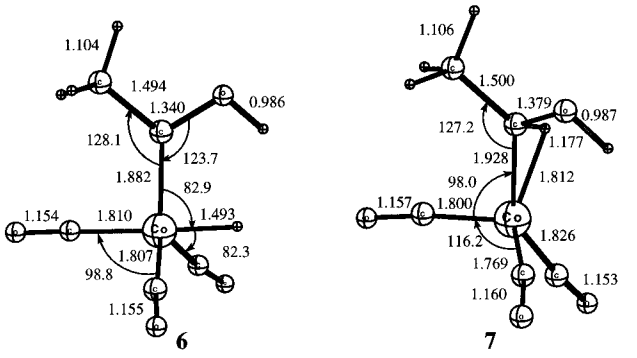

Figure 4. Optimized structures for complexes **6** and **7**. Bond distances are in Å, and angles are in deg.

inefficient type, **1c**, already encountered in TS(**2** → **4**). However, the barrier for the **2** → **6** paths is higher than for the **2** → **4** step. This is so, since the H_2 molecule in order for one of the hydrogens to reach the acyl oxygen is further away from the metal center.

We have also traced the energy profile for the **3** → **6** transit starting from complex **3** and using the O−H bond formed as the reaction coordinate, although in this case the hydrogen is not directly transferred to the oxygen atom but rather goes first to the carbon atom yielding complex **4**, **3** → **4** of Figure 3, followed by a migration of hydrogen from carbon to oxygen on the acyl group, **4** → **6** of Figure 3. In a direct transfer of hydrogen the Co−H bond would presumably have to be nearly broken before a O-H bond could be formed.

The exothermic **3** → **4** transit has already been discussed. It has a low barrier of 10 kJ·mol^{-1} and is quite feasible. The energy profile corresponding to the **4** → **6** process has an energy barrier as high as 172.0 kJ·mol^{-1}, and therefore this interconversion is not possible at room temperature. The high barrier for **4** → **6** is associated with the strain in the three-center transition state TS(**4** → **6**) of Figure 3. In orbital terms this translates into poor bonding overlaps between $1s_H$ and the σ-orbitals on oxygen and carbon of the acyl groups since these orbitals are unable to direct themselves straight toward the hydrogen atom.

To sum up, the hydroxycarbene complex **6** is kinetically only accesible at high temperatures, and it is unlikely that significant concentrations of this intermediate are present under normal hydroformylation conditions. Nevertheless, if obtained, complex **6** would be easily transformed to complex **7**, since the **6** → **7** conversion has a calculated energy barrier of only 6.6 kJ·mol^{-1}. The pseudotetrahedral complex **7** is the most stable among the **2**−**7** systems. It has a marked agostic interaction in which the Co−H bond distance is 1.812 Å and the C−H bond length is 1.177 Å; see Figure 4.

The alternative pathway to the hydroxymethyl complex **7,** starting from the aldehyde π-adduct **5**, has been discussed in details elsewhere.[7d] The energy barrier for this process is a modest 42.7 kJ·mol^{-1}. Thus it is clear that the migratory insertion step **5** → **7** represents a more facile path to the hydroxymethyl complex **7** than any of the processes involving the hydroxycarbene intermediate **6**.

We shall finally briefly discuss the conversion of **7** to alcohol and the $HCo(CO)_3$ catalyst. The relative energies for the species involved are compiled in Table 2. Complex **7** can easily add H_2 to yield complex **8** in a process which is exothermic by 28.5 kJ·mol^{-1}, despite the fact that the Co−H agostic interaction is lost in complex **8**. It is expected that during the initial interaction between H_2 and complex **7** a rearrangement of the CO ligands will occur to leave complex **8** in its most stable conformation.[7d] We note that the process **7** + H_2 → **8** is more exothermic than the analogous reaction **1** + H_2 → **2**. This can be rationalized by observing that the hydroxymethyl group, $CH_3(H)C(OH)$, in **8** is less electron withdrawing than the acyl fragment CH_3CO in **2**. Thus the back-donation to $\sigma^*_{H_2}$ in **8** is more pronounced and stabilizing. It is in line with this argument that the H−H distance is larger in **8** than in **2,** 0.851 Å in complex **8** vs 0.826 Å in **2**. Also the H_2 fragment charge is 0.130 e$^-$ in complex **8** vs 0.164 e$^-$ in complex **2**. The molecular structure of **8** and those of complexes **9** and **10** are drawn in Figure 5.

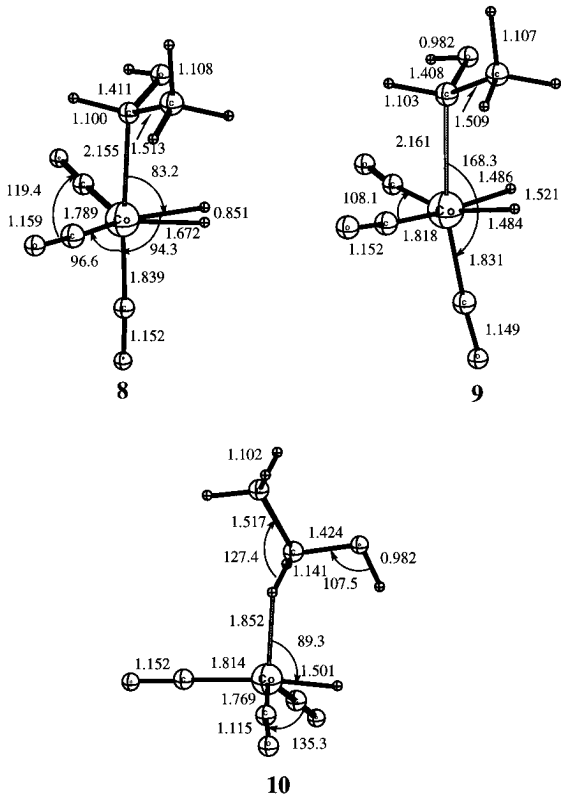

Figure 5. Optimized structures for complexes **8**−**10**. Bond distances are in Å, and angles are in deg.

Table 2. Relative Energies[a] for the Species Involved in H_2-Induced Ethanol Elimination

species	rel energy	species	rel energy
7 + H_2	28.5	TS(**8** → **9**)[b]	24.8
8	0	TS(**8** → **10**)[b]	49.8
9	24.8	TS(**9** → **10**)[b]	44.5
10	−30.1	CH_3CH_2OH + $HCo(CO)_3$	4.8

[a] All energies in kJ·mol^{-1} are relative to **8**. [b] The energy of the approximate transition state TS(**a** → **b**) is taken from the highest energy point on the linear transit **a** → **b**.

Complexes **8**−**10** are equivalent to complexes **2**−**4**, respectively, the only difference being the substitution of a hydroxymethyl group, $CH_3(H)C(OH)$, by an acyl fragment, CH_3CO. As before, complex **10** can be obtained by two different reaction paths: the oxidative addition/reductive elimination and the four-center transition state pathways. The former has an energy barrier of 44.8 kJ·mol^{-1}, whereas for the latter the energy

barrier is 49.8 kJ·mol^{-1}. The oxidative addition/reductive elimination reaction route (**8** → **9** → **10**) is again more favorable than the four-center transition state pathway (**8** → **10**), although the energy difference between these two pathways is now smaller, and therefore both mechanisms can be operative in this case.

The energy barrier for the four-center transition state pathway **8** → **10** is lower than for the corresponding **2** → **4** process on account of the fact that back-donation to $\sigma^*_{H_2}$ is more facile with the hydroxymethyl group, $CH_3(H)C(OH)$, than the acyl fragment, CH_3CO, as argued above. For the same reason, in the oxidative addition/reductive elimination reaction pathway (**8** → **9** → **10**) the activation energy for the addition step **8** → **9** of 24.8 kJ·mol^{-1} is lower than the barrier of 30.5 kJ·mol^{-1} calculated for the corresponding step **2** → **3** in the addition/reductive elimination reaction pathway (**2** → **3** → **4**). For the reductive elimination part, **9** → **10** has a barrier of 19.7 kJ·mol^{-1}, 9.2 kJ·mol^{-1} higher than **3** → **4** with 10.5 kJ·mol^{-1}. Now the superior electron-withdrawing ability of CH_3CO is better able to redistribute the electron density left on the metal from the reduction.

The geometrical changes undergone by complexes **8**−**10** during these transits are similar to those experienced by complexes **2**−**4**. Thus, from **8** to **9** there is a significant closing of the $CO_{ax}CoC_{acyl}$ and $CO_{eq}CoCO_{eq}$ angles, and also in the linear transit from **8** or **9** to **10** there is a rearrangement of the coordinated CO ligands to leave the hydride in an axial position of the TBP.

Finally, elimination of ethanol from complex **10** it is found to be an endothermic process by 34.9 kJ·mol^{-1}, but as in the release of acetaldehyde, this elimination will be facilitated by the formation of the $HCo(CO)_4$ species.

Concluding Remarks

In this work, we have shown that the hydrogenation of the 16-electron coordinatively unsaturated $CH_3(O)CCo(CO)_3$ species to produce acetaldehyde proceeds through the oxidative addition/reductive elimination pathway (**2** → **3** → **4**) with an energy barrier of only 36.3 kJ·mol^{-1}. The hydrogenation via a four-center transition state (**2** → **4**) is less likely, since it has a larger energy barrier of 70.4 kJ·mol^{-1}.

The generation of alcohol as a side product in the hydroformylation process was also considered. It was found that alcohol production is most likely to take place after aldehyde has been generated as an adduct in the π-complex $HCo(CO)_3(\eta^2\text{-}CH_3C(O)H)$, **5**. The first step is an isomerization of **5** to the hydroxymethyl species **7,** which after further hydrogenation can produce alcohol, Scheme 2.

We have also considered an alternative route to the key intermediate **7** and alcohol production without prior aldehyde generation. In this mechanism hydrogenation of the 16-electron coordinatively unsaturated $CH_3(O)CCo(CO)_3$, **1**, species leads to the hydroxycarbene intermediate **6** rather than aldehyde and $HCo(CO)_3$. Subsequently **6** could isomerize to the key intermediate **7**. It was found that **6** is thermodynamically accessible from **1** and H_2. However, the kinetic barrier associated with the process **1** + H_2 → **6** was estimated to be 96 kJ·mol^{-1} or more. This makes it unlikely that **6** is formed in significant quantities under normal hydroformylation conditions.

Acknowledgment. This investigation was supported by the Natural Sciences and Engineering Research Council of Canada (NSERC). We also acknowledge access to the IBM-RISC/6000 installations at the University of Calgary. M.S. acknowledges financial support provided by the Spanish Ministerio de Educación y Ciencia through DGICYT Contract No. PR95-110.

OM950881W